

See discussions, stats, and author profiles for this publication at: <https://www.researchgate.net/publication/297259901>

The Torque Rudder: A Novel Semi-Passive Actuator for Small Spacecraft Attitude Control

Conference Paper · August 2013

CITATIONS

2

READS

1,258

4 authors, including:



Grant Bonin

Deep Space Industries

21 PUBLICATIONS 64 CITATIONS

[SEE PROFILE](#)



Vincent Tarantini

University of Toronto Institute for Aerospace Studies

5 PUBLICATIONS 13 CITATIONS

[SEE PROFILE](#)



Robert E. Zee

University of Toronto

73 PUBLICATIONS 1,069 CITATIONS

[SEE PROFILE](#)

Some of the authors of this publication are also working on these related projects:



Science Knowledge Gaps for Asteroid Mining [View project](#)

The Torque Rudder: A Novel Semi-Passive Actuator for Small Spacecraft Attitude Control

Grant Bonin, Vincent Tarantini, Luke Stras, and Robert E. Zee
UTIAS Space Flight Laboratory
Toronto, On. Canada M3H 5T6; +1 (416) 667-7873
gbonin@utias-sfl.net; www.utias-sfl.net

ABSTRACT

This paper presents a novel concept for a semi-passive small spacecraft actuator. The proposed device consists of a set of solar cells that drive a small magnetic torquer automatically when illuminated. This device—referred to as a “torque rudder”, given its originally intended application in solar or drag sail missions—would be deployed or pre-positioned to automatically generate a magnetic disturbance torque proportional to its illumination. When the rudder is not illuminated, its residual magnetic moment would be zero, and the device would generate no torque. Thus, the proposed actuator has applications where sun-avoiding attitudes are desired in the absence of spacecraft commandability, and where permanent or bus-driven magnetic solutions are undesirable or unavailable. This paper describes the torque rudder concept, including a simple electrical and dynamic model for its use, with sample simulations derived from the CanX-7 drag sail deorbiting mission. A practical implementation is presented that enables sun-excluding modes for low-Earth orbit spacecraft with any LTAN. It is concluded that the torque rudder concept represents a novel, simple actuator when passive sun-pointing or sun-exclusion is desired, as may be the case for many small satellites.

BACKGROUND AND MOTIVATION

Many spacecraft have mission-critical constraints on attitude. There are several examples of spacecraft that are essentially constrained to “point or die”—spacecraft that must establish pointing control immediately following deployment in order to ensure or avoid a particular attitude. Usually, the pointing constraint is that the spacecraft must either maintain or avoid pointing at the sun. In the former case, this would be required for spacecraft that are not able to generate power in all attitudes, and must therefore align their solar panels with the sun to avoid completely draining the spacecraft batteries, which may constitute a loss-of-mission. In the latter case, a sensitive payload (particularly imaging payloads) may not be able to experience sustained (or even transient) sun stares without damage. In still other applications, such as solar sail missions, a sunward attitude may be necessary to maintain attitude and/or position control, while conversely, deorbiting drag sails [1,2] may wish to avoid sustained sun stares that may lock them into sub-optimal attitudes from the standpoint of generating aerodynamic drag.

Of course, many spacecraft with such attitude constraints are designed to deal with them. Many spacecraft have been launched that establish pointing for power generation immediately. Optical missions (space telescopes and Earth observation missions) have been launched with doors or shutters to avoid

accidental sun exposure, albeit at the expense of increased complexity. Solar and drag sail missions—a large number of which can be expected to launch over the coming decade [1,2]—have varying ways of dealing with their attitude constraints, from steerable thin-film structures to adaptive centre-of-pressure/centre-of-mass offsets to ensure proper steering [2].

This paper describes an innovation which the authors refer to as a “torque rudder”—so named because its genesis comes from efforts to avoid sun-facing attitudes for the CanX-7 drag sail mission [1] in a way that is simple and passive. While not ultimately required or used on CanX-7, it was recognized that the torque rudder concept may prove useful for other low-Earth orbit (LEO) satellites with sun-avoidance attitude constraints, where it may be more robust and/or cost-effective to establish such constraints passively, without the satellite needing its attitude control system to be “all-up” shortly after launch.

TORQUE RUDDER OVERVIEW

The concept of photo-sensitive attitude actuators has been described before—in reference [3], a photochemical micro-thruster is considered for attitude control. The torque rudder concept, however, has the benefit of being a passive and non-perishable actuator, in the sense that its action is both automatic and does not employ any consumables.

The torque rudder idea is conceptually straightforward. It consists of a small solar cell (or solar cell string) that drives a small magnetic torquer automatically when illuminated. Depending on the orientation of the solar cell with respect to the torquer (and the torquer with respect to the geomagnetic field) a disturbance torque proportional to illumination—that is, proportional to sunward attitude—is generated by the rudder. When not illuminated, the magnetic moment of the rudder goes to zero, eliminating the disturbance—thus, the torque rudder does not have a permanent magnetic dipole that may otherwise disturb satellite attitude control sensors or actuators. Thus, depending on orientation, the torque rudder can be used to avoid a sun-facing attitude. While the concept described was originally intended to aid spacecraft in sun avoidance, the same principle (and hardware) may also be used to perform coarse sun tracking in some orbits and spacecraft configurations (though this is not generally true, and depends on circumstances)—useful for spacecraft that may need to maintain illumination but wish to avoid the challenge of establishing attitude control immediately following deployment.

A Simple Model

A simple model of the torque rudder is presented below. Consider a simple magnetorquer design (air core) with n turns and A enclosed area, driven by a solar cell with a peak current I_{sc} . The magnetic moment generated, m (Am^2), by the torquer will be proportional to the angle between the solar cell and the sun, θ , according to:

$$m = nAI_{sc} \cos \theta$$

Figure 1 shows the magnetic moment generated by a reference torque rudder design with a circular enclosed area of 0.0013 m^2 (i.e. a 4 cm inner diameter) and a solar cell with 0.5A peak current, on lines of constant number of turns. As can be observed from Figure 1, substantial dipoles (and correspondingly, substantial disturbances) can be generated by a torque rudder when illuminated, with the residual magnetic moment falling to zero when not illuminated. As described, the dipole generated is proportional to illumination. This model does not assume any core material for the purposes of simplicity—the actual hardware concept (described in the following section) would use iron core material to further increase the dipole generated, which can be used to trade off number of windings, power consumption, and size against dipole.

In reality, solar cells follow a Kelly cosine characteristic, rather than a regular cosine characteristic, with current output falling exponentially

beyond roughly 60° . This is even further beneficial for the torque rudder concept, but is not assumed for the purposes of this simple analysis. (Figure 2 illustrates the difference between the cosine and Kelly cosine for reference.)

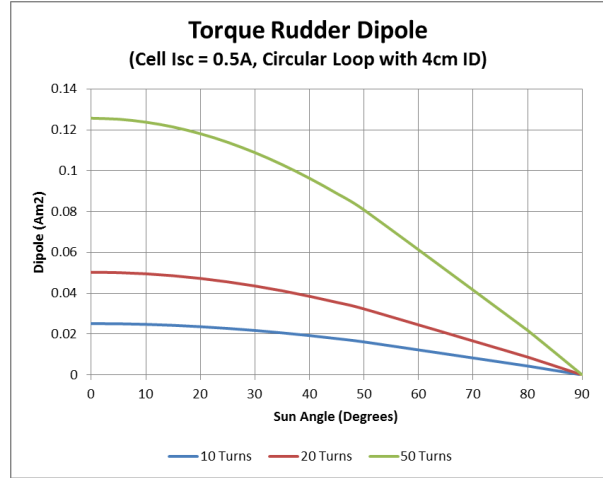


Figure 1: Simplified Torque Rudder Performance on Lines of Constant Turns

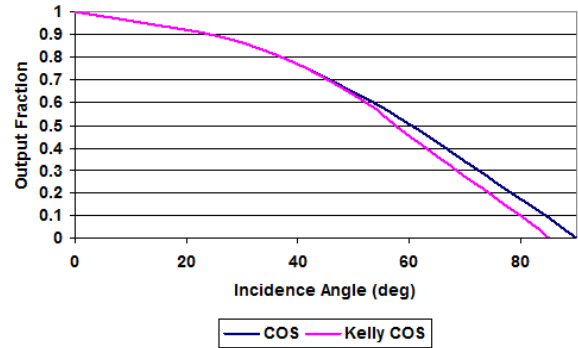


Figure 2: Comparison of Cosine and Kelly Cosine Characteristics

It should be noted that in order for the torque rudder to function as described, the dipole generated must produce torque by interacting with the Earth's magnetic field. The extent to which the approach is effective will therefore depend somewhat on inclination. In this paper, we only consider high inclination (sun synchronous) orbits. For reference, Figure 3 shows the orientation of the magnetic field in the plane of a polar sun synchronous orbit.

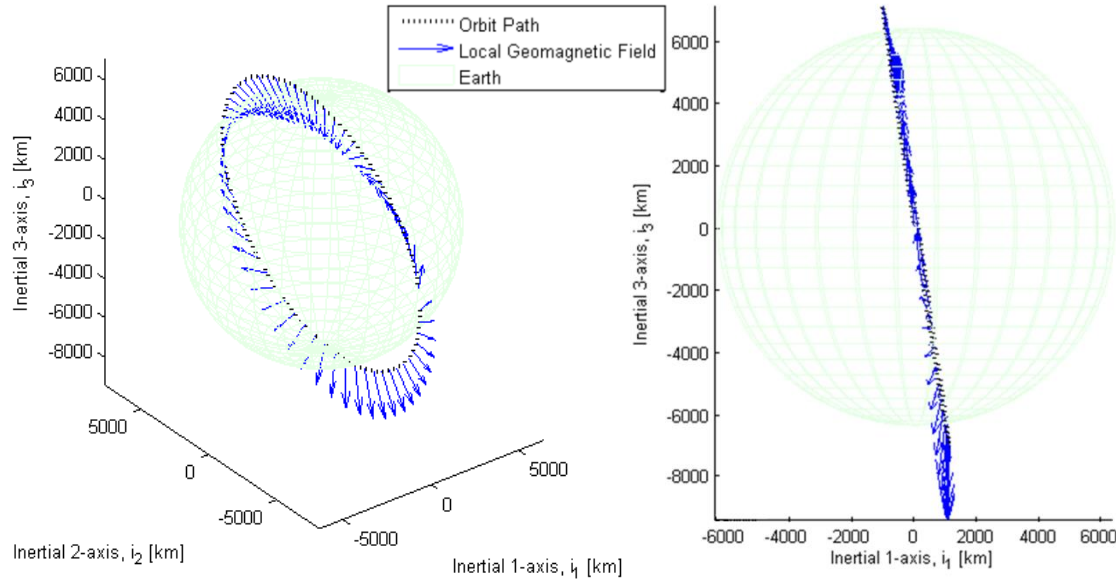


Figure 3: Orientation of Local Geomagnetic Field in SSO Orbit Plane

HARDWARE IMPLEMENTATION

Figure 4 illustrates the torque rudder concept reference design. The torque element is shown sectioned, with an iron core and copper windings visible. The torque element in this case is powered by a 1 W solar cell, which can be positioned as required, without additional

device-level constraints on the spacecraft. Wires connecting the solar cell to the torque element are of arbitrary length, and may be sized to suit the spacecraft mechanical design. Blocking diodes, if required, are on the back of the solar cell. The magnetic field generated by the torque rudder under full illumination conditions is illustrated in Figure 5.

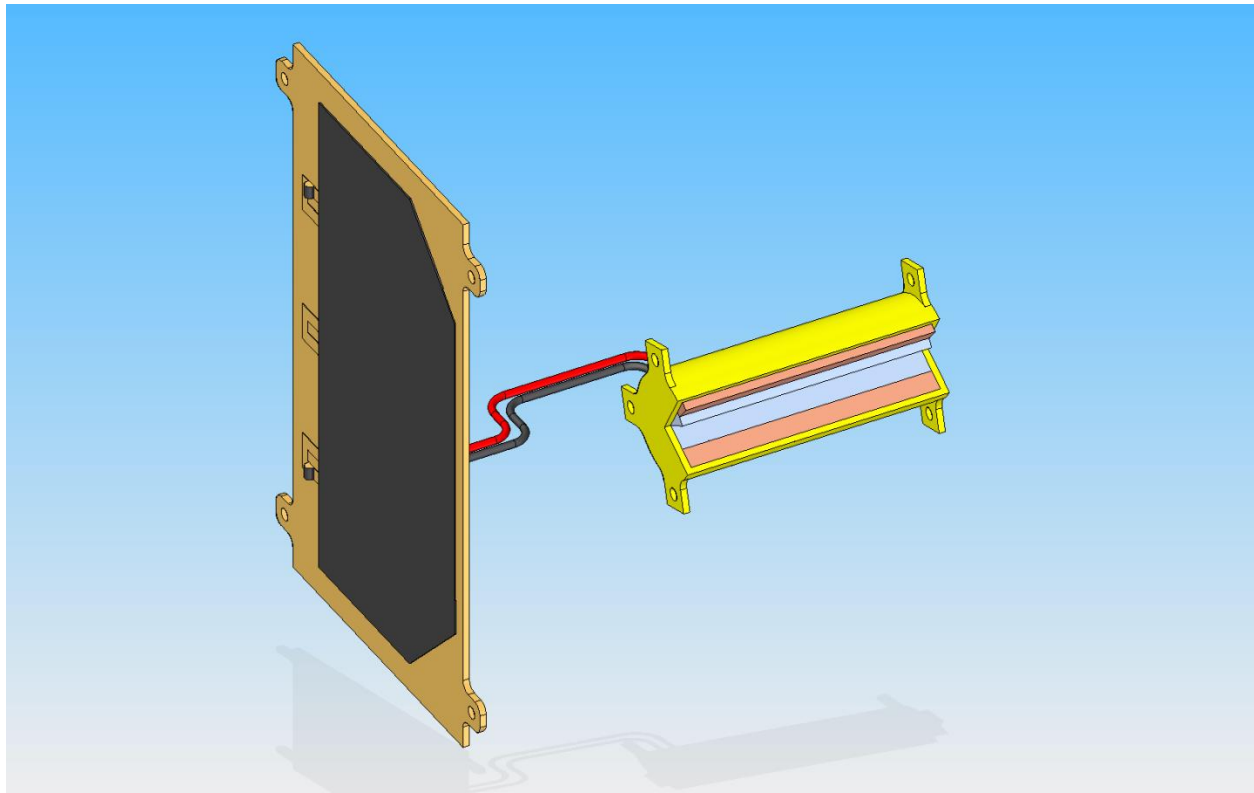


Figure 4: Torque Rudder Concept

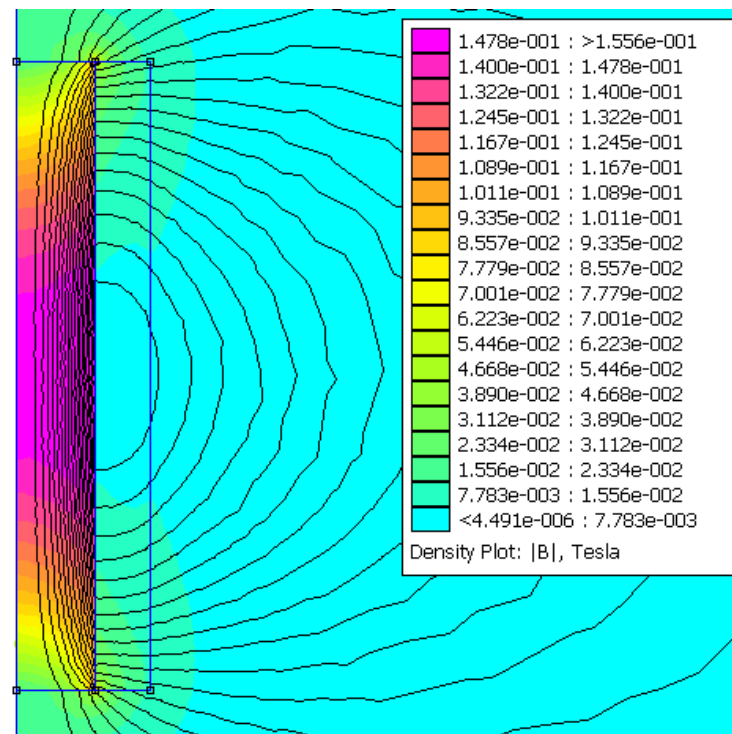


Figure 5: Magnetic Field Density Plot for Torque Rudder Reference Design, Full Illumination

A spacecraft using the torque rudder design shown in Figure 4 would mount the solar cell and torquer as required to generate the required disturbance torque when illuminated.

DETAILED DYNAMICS MODEL

Following from the simplified model presented earlier, we now describe a complete dynamics model for the torque rudder.

The rotational dynamics of a rigid body behave according to Euler's equations:

$$I\dot{\omega} + \omega \times I\omega = \mathbf{G}$$

Where the total applied torque \mathbf{G} is comprised of the torque due to gravity gradient \mathbf{G}_g , solar radiation pressure \mathbf{G}_s , geomagnetic \mathbf{G}_m , and aerodynamic \mathbf{G}_a . The geomagnetic disturbance may be further broken down into two components:

$$\mathbf{G}_m = \mathbf{G}_{mr} + \mathbf{G}_{mc}$$

Where, \mathbf{G}_{mr} is the disturbance caused by the spacecraft's residual magnetic field, and \mathbf{G}_{mc} is the control torque induced by the torque rudder. The control torque \mathbf{G}_{mc} is the result of the interaction between the torque rudder's magnetic coil and Earth's magnetic field. When a current is running through the coil, a magnetic field is created in accordance with the Biot-Savart Law. The offset between Earth's magnetic field and the coil's field causes a torque to be applied to the spacecraft acting to bring the two fields into alignment.

The magnetic field created within the torque rudder coil can be modeled as a magnetic dipole moment \mathbf{m}_c whose magnitude is directly dependent upon the current i through the coil:

$$\mathbf{m}_c = k_c i(\theta) \hat{\mathbf{n}}_c$$

Where, k_c is the coil loop-area product (equivalent number of loops within the coil multiplied by the average loop area) and $\hat{\mathbf{n}}$ is the normal vector for the coil. The control torque induced by the interaction between the coil's magnetic dipole moment \mathbf{m}_c and Earth's magnetic field \mathbf{B} is then defined as:

$$\mathbf{G}_{mc} = \mathbf{m}_c \times \mathbf{B}$$

The current is being driven through the coil by a dedicated solar array; when the solar array is illuminated, it drives a current through the coil. By orienting the torque rudder's coil and solar array in an appropriate arrangement, the torque rudder can be used

to achieve one or more of the applications described at the beginning of this paper.

TORQUE RUDDER SIZING

In order to size the torque rudder, the worst-case disturbance environment is considered. There are four major attitude disturbance sources to account for in the LEO environment, as presented previously—gravity gradient, geomagnetic, solar radiation pressure, and aerodynamic. Here we use estimates of the worst-case magnitude of each disturbance source to size the torque element of the rudder.

The magnitude of the gravity gradient disturbance is defined as follows:

$$||\mathbf{G}_g|| = \frac{3\mu}{2R^3} \Delta I$$

Where, $\mu = 3.986 \times 10^{14} \text{ m}^3 \text{ s}^{-2}$ is Earth's gravitational parameter, R is the distance of the satellite from the centre of Earth, and ΔI is the difference between principal inertias.

The magnitude of the geomagnetic disturbance caused by the residual magnetic field within the spacecraft is simply the product of the magnitudes of the expected residual dipole \mathbf{m}_r and Earth's magnetic field \mathbf{B} :

$$||\mathbf{G}_{mr}|| = ||\mathbf{m}_r|| ||\mathbf{B}||$$

The magnitude of the disturbance torque caused by solar radiation pressure is defined by the following where $p = 4.563 \times 10^{-6} \text{ N} \cdot \text{m}^{-2}$ is the nominal solar radiation pressure acting on a surface at 1 AU, A is the total area of the illuminated surfaces, and L_{cp_s} is the offset between the centre of mass of the satellite and the centre of solar pressure of the illuminated surfaces:

$$||\mathbf{G}_s|| = \frac{1}{2} p A L_{cp_s}$$

The magnitude of the aerodynamic disturbance is defined by the following equation. ρ is the total atmospheric density (which varies substantially both short- and long-term in LEO), v is the satellite's speed, C_D is the drag coefficient, A is the total area of the surfaces exposed to the flow, and L_{cp_a} is the distance between the satellite's centre of mass and the centre of aerodynamic pressure of the exposed surfaces:

$$||\mathbf{G}_a|| = \frac{1}{4} \rho v^2 C_D A L_{cp_a}$$

In general, the described disturbance torques will be acting in arbitrary directions resulting in a net torque

which is less than the sum of the magnitudes of each individual disturbance. However, for sizing purposes, it is conservatively assumed that the disturbances are combined linearly. In addition, the magnitude of the control torque is required to be twice the maximum expected disturbance when the coil's magnetic dipole moment is oriented at 45° with respect to Earth's local geomagnetic field:

$$||\mathbf{m}_c||_{required} = \frac{2\sqrt{2}||\mathbf{G}_{max}||}{||\mathbf{B}_{max}||}$$

CASE STUDIES

To illustrate the utility of the torque rudder in “real” missions, we consider two different spacecraft designs and sets of attitude constraints as examples. In particular, these cases are:

- **Case A:** a small triple cubesat with a 4m^2 deorbiting drag sail (similar to the CanX-7 mission), which must avoid sunward attitudes in order to create aerodynamic drag (“spacecraft A”); and
- **Case B:** an 80 kg Earth observation (EO) microsatellite, which must avoid pointing its instrument aperture at the sun for extended durations (“spacecraft B”)

In Scenario A, a 3U satellite has reached end of life and has deployed a 4 m^2 drag sail to de-orbit. In certain orbits (i.e. dawn-dusk), and if the spacecraft has an unfavorable residual magnetic moment, it risks becoming locked in a “sail edge-on” attitude. Under these circumstances, in which the drag sail plane is parallel to the velocity vector, little drag would be generated as a result. In this case, the torque rudder is used to ensure that the edge-on attitude is unsustainable.

In Scenario B, an 80 kg EO microsatellite is studied, in which the satellite has an optical instrument that cannot tolerate sustained sun stares without damage. It is undesirable to require spacecraft attitude control immediately following launch, and mechanical doors or shutters are considered high-risk options to mitigate sun stares. In this case, the torque rudder is used to avoid long-duration sunward attitudes.

Performance Metrics

To demonstrate the effectiveness of the torque rudder, each scenario was simulated with and without the

proposed device. The metrics used to describe the attitude response are defined as follows:

$$\eta_{aero}(t) = |\hat{\mathbf{v}}(t) \cdot \hat{\mathbf{d}}| \quad \eta_{mag}(t) = |\hat{\mathbf{B}}(t) \cdot \hat{\mathbf{m}}(t)|$$

$$\eta_{sun} = |\hat{\mathbf{s}}(t) \cdot \hat{\mathbf{d}}|$$

Where, $\hat{\mathbf{d}}$ is the satellite body vector of importance. For Scenario A, $\hat{\mathbf{d}}$ is the drag sail normal vector (corresponding to the spacecraft body y-axis in Figure 6. For Scenario B, $\hat{\mathbf{d}}$ is the normal vector of the small face of the satellite (corresponding to the spacecraft body x-axis in these analyses), $\hat{\mathbf{m}}$ is the direction vector of the total spacecraft magnetic dipole moment including both the residual dipole and the one resulting from the torque rudder, $\hat{\mathbf{v}}$ is the velocity vector, $\hat{\mathbf{B}}$ is the local geomagnetic field, and $\hat{\mathbf{s}}$ is the sun vector. When the metric is unity, $\hat{\mathbf{d}}$ is aligned with the respective environment vector, when the metric is zero, the two vectors are perpendicular to each other. A sustained value close to one indicates that the spacecraft has settled into an aerodynamic-, magnetic-, or sun-stabilized attitude. Another set of metrics are defined to summarize the attitude behavior which are simply the time-averages of the metrics defined above:

$$\gamma_{aero} = \int_0^T \frac{\eta_{aero}(t)}{T} dt \quad \gamma_{mag} = \int_0^T \frac{\eta_{mag}(t)}{T} dt$$

$$\gamma_{sun} = \int_0^T \frac{\eta_{sun}(t)}{T} dt$$

Where T is the total simulation time.

Case A: Triple-Cube Drag Sail Deorbiter

Scenario A was originally studied for the CanX-7 drag sail deorbiting mission during its preliminary design phase, when it was uncertain whether the spacecraft could become stuck in a “sail edge to velocity vector” orientation due to solar radiation pressure effects in a dawn-dusk sun synchronous orbit. Fortunately, the CanX-7 spacecraft and sail design are otherwise robust to this case, and no mitigation approaches such as the torque rudder were required. However, for similar missions that may wish to avoid requiring ACS functionality over the deorbiting phase, or for similar missions in general, the torque rudder is shown to be useful for creating sun-stare-proportional disturbances.

Table 1 summarizes key parameters for Spacecraft A, while Figure 6 illustrates the spacecraft geometry being considered in Case A.

Table 1: Scenario A Spacecraft Properties

Parameter	Value / Comment
Mass	4.5 kg
Inertia	$\begin{bmatrix} 0.2 & 0 & 0 \\ 0 & 0.3 & 0 \\ 0 & 0 & 0.2 \end{bmatrix} \text{ kg} \cdot \text{m}^2$
Bus Dimensions	0.3 m by 0.1 m by 0.3 m
Sail Dimensions	2.0 m by 2.0 m
Residual Magnetic Dipole Moment	$0.05 \text{ A} \cdot \text{m}^2$
Orbit	800 km sun-synchronous orbit with local time at the ascending node of 18:00

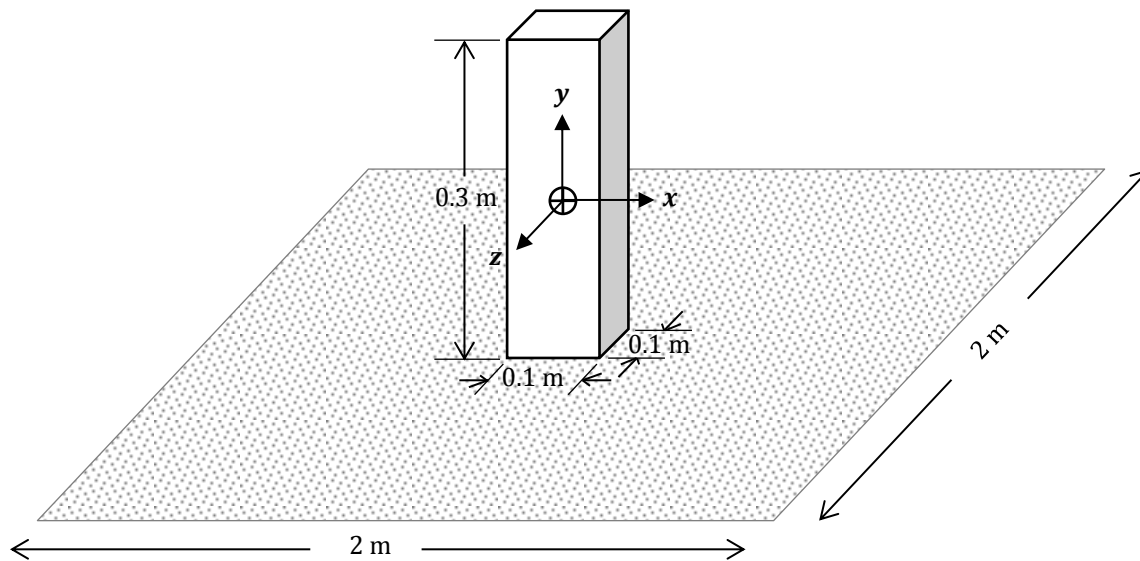


Figure 6: Spacecraft Configuration for Scenario A

Disturbance Environment and Rudder Sizing

The expected attitude disturbances described above can be estimated for Spacecraft A as follows, allowing the required torque rudder magnitude to be calculated.

For Scenario A, $\Delta I_{max} = 0.1 \text{ kg} \cdot \text{m}^2$. The orbit is assumed to be a circular orbit with an altitude of 800 km. The maximum magnitude of the gravity gradient disturbance is therefore:

$$||\mathbf{G}_g||_{max} = 0.16 \mu\text{N} \cdot \text{m}$$

The maximum expected residual magnetic dipole moment for Spacecraft A is assumed to be $0.05 \text{ A} \cdot \text{m}^2$. Earth's magnetic field reaches a maximum magnitude of $56 \mu\text{T}$ in low earth orbit. The maximum magnitude of the geomagnetic disturbance torquer is therefore:

$$||\mathbf{G}_{mr}||_{max} = 2.8 \mu\text{N} \cdot \text{m}$$

Considering the solar radiation pressure disturbance, for a 3U satellite with a 4 m^2 deployed drag sail, $L_{cps} = 0.15 \text{ m}$ and $A = 4.0 \text{ m}^2$. The resulting maximum magnitude of the solar radiation disturbance is therefore:

$$||\mathbf{G}_s||_{max} = 1.4 \mu\text{N} \cdot \text{m}$$

Lastly, for our 3U example, the following maximum values are assumed:

- $p_{max} = 1 \times 10^{-13} \text{ kg} \cdot \text{m}^{-3}$, corresponding to the maximum expected density at an altitude of 800 km.
- $v_{max} = 7452 \text{ m} \cdot \text{s}^{-1}$, corresponding to a satellite's speed in a circular orbit with altitude 400 km.
- $C_{D_{max}} = 2.2$
- $A = 4.0 \text{ m}^2$
- $L_{cpa} = 0.15 \text{ m}$

The maximum magnitude of the disturbance torque caused by aerodynamic drag using these parameters is:

$$||\mathbf{G}_a||_{max} = 1.8 \mu\text{N} \cdot \text{m}$$

With the resulting total disturbance torque calculated as:

$$||\mathbf{G}_{max}|| = 6.2 \mu\text{N} \cdot \text{m}.$$

Thus, the required dipole for the torque rudder coil for Satellite A is

$$\begin{aligned} ||\mathbf{m}_c||_{required} &= \frac{2\sqrt{2}||\mathbf{G}_{max}||}{||\mathbf{B}_{max}||} \\ &= \frac{2\sqrt{2}(6.2 \mu\text{N} \cdot \text{m})}{56 \mu\text{T}} \\ &= 0.31 \text{ A} \cdot \text{m}^2 \end{aligned}$$

Case A Simulation Results

In Case A, the 3U satellite with deployed drag sail is in a dusk-dawn sun-synchronous orbit. At high altitudes where the atmosphere is very thin, there may not be sufficient aerodynamic drag to achieve aero-stabilization. Instead, the spacecraft may become sun-stabilized since the sail surface is not a perfect mirror. In an orbit where the beta angle (the angle between the sun vector and orbit plane) is near 90° , a sun-stabilized attitude would result in a near minimum-drag attitude for the drag sail.

This degenerate attitude case for Scenario A is shown in Figure 7. By examining the response, it can easily be seen that the spacecraft has become almost completely sun-stabilized (indicated by $\gamma_{sun} \approx 1$). And, since the orbit beta angle is near 90° , the resulting γ_{aero} is only 16.6 %: that is, the drag sail is being prevented from projecting anywhere near its maximum area in the velocity vector, reducing its efficacy substantially.

Figure 8 shows the difference in response when a torque rudder is used. The results show that the torque rudder has effectively eliminated the ability of the spacecraft to become sun-stabilized; rather, the spacecraft with torque rudder tends towards a magnetic-stabilized attitude profile, which is much better for drag sail projected area in this case. The resulting γ_{aero} is 44.6 %, which is approximately 2.7 times better.

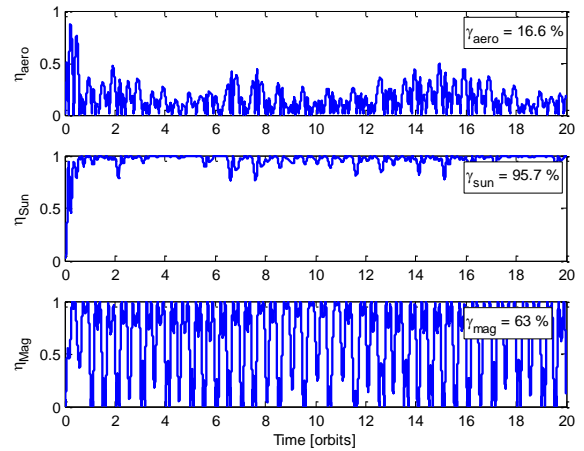


Figure 7: Case A Attitude Response – No Torque Rudder

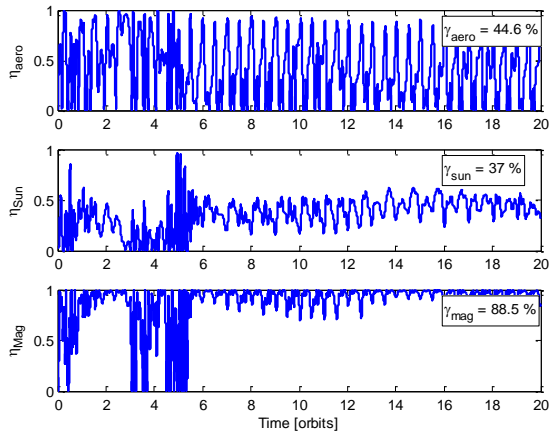


Figure 8: Case A Attitude Response – With Torque Rudder

Case B: Earth Observation Microsatellite with Sun Stare Constraint

In Case B, an 80 kg microsatellite with a sun avoidance attitude constraint is considered. This class of satellite is increasingly common, with the principle application being Earth Observation (EO). In many cases, EO missions cannot tolerate sustained sun stares with their instruments, as discussed previously—thus, in this scenario, the torque rudder is used to disturb the satellite from sunward attitudes in the absence of attitude control authority from the bus. No assumptions are made about instrument field of view (FOV)—instead, we simply evaluate the angle between the sun and panel normal where the instrument aperture is assumed to be located (i.e. the instrument boresight). Table 2 summarizes the spacecraft properties assumed in Case B, while Figure 9 provides an illustration of the assumed satellite geometry.

Table 2: Spacecraft Properties

Parameter	Spacecraft B
Mass	80 kg
Inertia	$\begin{bmatrix} 2 & 0 & 0 \\ 0 & 3 & 0 \\ 0 & 0 & 4 \end{bmatrix} \text{ kg} \cdot \text{m}^2$
Bus Dimensions	0.5 m by 0.4 m by 0.3 m
Sail Dimensions	No sail
Residual Magnetic Dipole Moment	$0.45 \text{ A} \cdot \text{m}^2$
Orbit	800 km sun-synchronous orbit with local time at the ascending node of 18:00

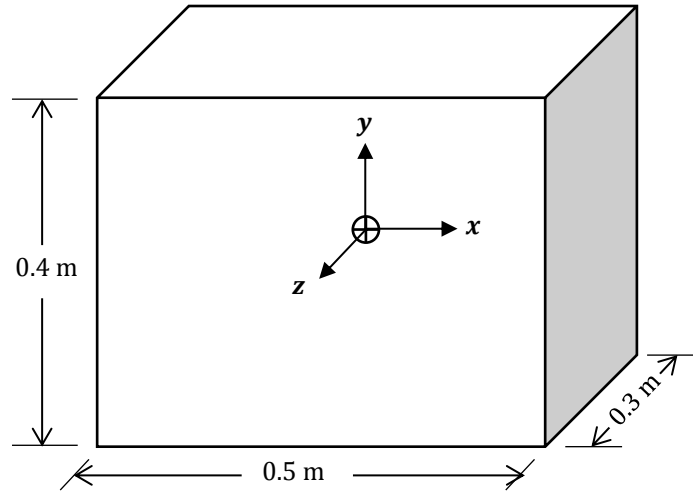


Figure 9: Spacecraft B

Disturbance Environment and Rudder Sizing

The expected attitude disturbances for Case B are estimated below. Once the total maximum disturbance is determined, the required torque rudder magnitude is calculated, as in the previous case.

Considering gravity gradient disturbances, the maximum difference in principal inertias for Satellite B is $2 \text{ kg} \cdot \text{m}^2$. The maximum magnitude of the gravity gradient disturbance is therefore:

$$||\mathbf{G}_g||_{\max} = 3.2 \text{ } \mu\text{N} \cdot \text{m}$$

The maximum residual dipole moment is assumed to be $0.45 \text{ A} \cdot \text{m}^2$. The maximum magnitude of the geomagnetic disturbance is therefore:

$$||\mathbf{G}_{mr}||_{\max} = 25.2 \text{ } \mu\text{N} \cdot \text{m}$$

For Satellite B, the disturbance caused by solar radiation pressure is effectively negligible compared to the geomagnetic and gravity gradient disturbances. This is because the satellite is approximately symmetric about the centre of mass in any orientation. This is unlike Satellite A which has a large exposed area (the drag sail) on one side of the centre of mass. The disturbance caused by aerodynamic drag is also effectively negligible. It is therefore ignored in defining the overall disturbance magnitude.

The resulting total disturbance torque is:

$$||\mathbf{G}_{\max}|| = 28.4 \text{ } \mu\text{N} \cdot \text{m}.$$

And the required dipole for the torque rudder coil for Satellite A is

$$\begin{aligned} ||\mathbf{m}_c||_{\text{required}} &= \frac{2\sqrt{2}||\mathbf{G}_{\max}||}{||\mathbf{B}_{\max}||} \\ &= \frac{2\sqrt{2}(28.4 \text{ } \mu\text{N} \cdot \text{m})}{56 \text{ } \mu\text{T}} \\ &= 1.43 \text{ A} \cdot \text{m}^2 \end{aligned}$$

This too can be accomplished readily using the reference design described earlier.

Case B Simulation Results

In Scenario B, the spacecraft is assumed to have entered a minor axis spin at a rate of 6 deg/s , such that the instrument aperture is pointed towards the sun in a relatively stable attitude. The attitude response is shown in Figure 10. Figure 10 indicates that the time-average angle between the instrument boresight and solar vector is approximately $\cos^{-1}(0.949) = 18^\circ$, which would be within the FOV of many instruments and is considered to be a sustained sun stare in this analysis. Stuck in this minor axis spin, an instrument that cannot tolerate sustained sun stares would certainly experience damage.

Fortunately in this case, with the introduction of a torque rudder, the spacecraft is unable to sustain the minor axis spin. The results, shown in Figure 11, show how the torque rudder disturbs the satellite away from its sunward attitude once activated—the instrument

cannot remain sunward with the torque rudder employed. The time-average angle between the sun vector and small face normal is $\cos^{-1}(0.197) = 79^\circ$ —that is, even instruments with wide-angle FOVs would avoid sustained sun stares in this configuration.

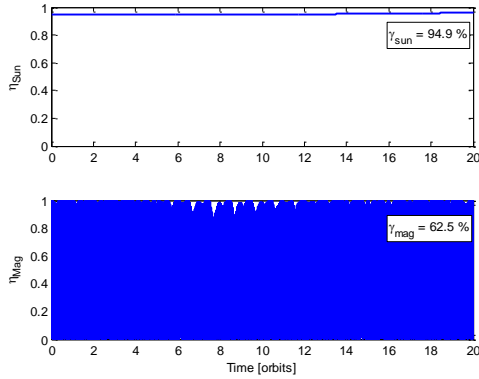


Figure 10: Nominal response for Scenario B

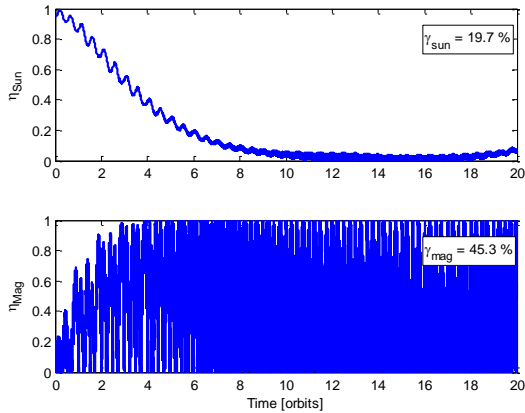


Figure 11: Response for Scenario B with the torque rudder

While sustained sun stares are successfully avoided using the torque rudder, it is noteworthy that transient attitudes—in which the solar vector briefly passes through the instrument FOV—may still occur. To examine this, we consider the case of a random tumble, and evaluate the number of consecutive minutes during which the solar vector is within a given FOV with and without the torque rudder used. In these simulations, the spacecraft is assumed to be in a random tumble initially, and the consecutive minutes sunward vs. FOV is evaluated with and without the torque rudder over time. These simulations are summarized in Figure 12. The results show that sun avoidance is drastically improved by the torque rudder, reducing the length of

consecutive time that the sun is within specific FOVs by up to 90 %.

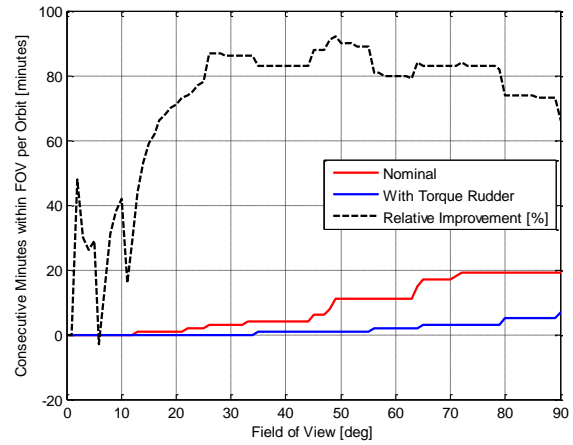


Figure 12: Sun Stare Duration vs. FOV—With and Without Torque Rudder

CONCLUSIONS

For spacecraft with mission-critical attitude constraints—such as sail missions and earth observation missions, both discussed above—the torque rudder concept presented in this paper offers an alternative to the “point or die” approach taken on many satellites. The torque rudder concept described here can be used to automatically generate a magnetic disturbance proportional to illumination, and thus can be used where sun-avoiding attitudes are desired in the absence of bus-side attitude control.

In this paper, we have presented a high-level overview of the torque rudder principle and concept, and evaluated its utility to both drag sail and Earth observation case studies. It is concluded that the torque rudder concept represents a novel, simple actuator when passive sun-pointing or sun-exclusion is desired, as may be the case for many different LEO satellites.

ACKNOWLEDGEMENTS

The authors would like to thank the CanX-7 funding partners—the National Sciences and Engineering Research Council (NSERC), Defence Research and Development Canada, Ottawa Branch (DRDC Ottawa), and COM DEV. Although the innovation described in this paper is not intended to be used on the CanX-7 mission itself, the genesis of the concept was from the CanX-7 preliminary design.

REFERENCES

- [1] G. Bonin, J. Hiemstra, T. Sears, and R. E. Zee, “The CanX-7 Drag Sail Demonstration Mission: Enabling Environmental Stewardship for Nano- and Microsatellites”, 27th Annual AIAA/USU Conference on Small Satellites, SSC13-XI-9, August 2013.
- [2] V. Lappas, et al., “Demonstrator Flight Missions at the Surrey Space Centre involving Gossamer Sails”, 3rd International Symposium on Solar Sailing, University of Strathclyde, Glasgow, Scotland, June 2013.
- [3] J. N. Maycock and V. R. Pai Verneker, “A Photochemical Microrocket for Attitude Control”, *J. Spacecraft and Rockets*, V. 6, No. 3, pp. 336-337, March 1969.